Relationship between Composition and Structure in Chitosan-based Hybrid Films

S. Fuentes,[†] P. J. Retuert,[‡] A. Ubilla,[§] J. Fernandez,[§] and G. Gonzalez*[,†]

Department of Chemistry, Faculty of Science, University of Chile, Casilla 653, Santiago, Chile; Department of Chemistry, Faculty of Physical and Mathematical Science, University of Chile, Casilla 277, Santiago, Chile; and Laboratory of Developmental and Cell Biology, Department of Biology, Faculty of Science, University of Chile, Casilla 653, Santiago, Chile

Received January 21, 2000

Chitosan/poly(aminopropylsiloxane) hybrid films were obtained by blending 3-(aminopropyl)siloxane oligomers (pAPS) with chitosan (CHI). The pAPS oligomers were prepared by the sol−gel method starting from 3-(aminopropyl)triethoxysilane. These hybrids were characterized by chemical, spectroscopic and morphological methods. Scanning electron micrographs of hybrid films of different composition revealed an organized microscopic pattern suggesting the existence of systematic interactions among their components. Comparison of the thermal stabilities and X-ray diffraction patterns as well as FT-IR spectra of the films with those of the pure components revealed that nanocomposites were formed. Similar studies of films including lithium perchlorate, as a third component, showed that addition of certain amount of lithium ions affected the structure of the CHI/pAPS films. When addition of the lithium salt exceeded the homogeneous incorporation limit, a little excess generated anisotropically oriented patterns in the hybrid films.

Introduction

Study of hybrid nanocomposites arising from the compatibilization of organic and inorganic polymers has been an active research area in recent years.[1] Incorporation of organic polymers, especially those with amino or amide groups, into inorganic siliceous matrices allows the formation of molecular hybrids often stabilized by strong hydrogen bonding.[2] The use of sol−gel processes has been demonstrated to be very helpful to produce this type of materials under soft conditions (room temperature). Generation of inorganic networks at low temperatures permits us indeed to obtain an intimate mixture of both organic and inorganic components at the molecular level.[3−5] In recent years, incorporation of biopolymers into inorganic networks has generated increasing interest for the preparation of biomimetic materials.[6,7] The morphological characteristics of this type of hybrid materials are therefore of special relevance.[8,9] These kinds of organic−inorganic nanocomposites often display complex multifunctional structures potentially related to biomineralization processes.

We have been interested in the use of the biopolymer chitosan to prepare macromolecular organic−inorganic hybrids. Chitosan, poly-[(1−4)-2-amino-2-deoxy-D-glucose] (CHI), is produced by alkali metal treatment of chitin, an abundant polysaccharide contained in the shell (exoskeleton) that covers the crustacean body.[10] Nanoporous membranes prepared from chitosan have many technical and biomedical applications, mainly because of their bio- and hemocompatibility.[11−13] Although many applications of chitosan are related to what is known of its molecular and supramolecular organization, particularly of the crystalline structure of its films and membranes, we are still far from understanding the relationship between its molecular structure and function.

We have recently reported[14] that blending of chitosan (CHI) with poly(aminopropylsiloxane) (pAPS) in a 0.6:1 molar ratio produced a hybrid compound of singular behavior. This resulted in obtaining a molecular complex, which led to the formation of transparent and flexible films. In this work, we describe the morphology and crystallinity of these films, and also the effect of adding lithium perchlorate, that led to a new molecular complex with different properties.

Experimental Section

Chitosan (CHI) (Bioquimica Austral Ltd., Chile) was washed with acetone and methanol and dried to constant weight. Its molecular weight ($M_v = 3.5 \times 10^5$) was determined as previously described.[15,16] As estimated by ^{1}H NMR spectroscopy[17] the deacetylation degree of chitosan was estimated to be 87.5%. 3-(Aminopropyl)triethoxysilane (APS) from Aldrich was used. The pAPS solution was obtained by hydrolyzing APS in 0.5 M formic acid at 45 °C for 3 days; thereafter, the solvent was removed by evaporation until the solution stopped flowing. In this manner, a solution containing about 0.7 g of pAPS/mL was obtained. Analyzed by size exclusion chromatography (Bruker LC 21B with a Shodex OH pack 803-column), this solution contained aminopropylsiloxane oligomers (pAPS) with $M_w \approx 800$.

CHI and pAPS were used as 5% w/w formic acid solutions. To get films with a molar ratio of 0.6:1:0.8 (CHI:pAPS:Li), anhydrous

* To whom correspondence should be addressed. E-mail: ggonzale@uchile.cl. Fax: 56-2-671 3888.

[†] Department of Chemistry, Faculty of Science, University of Chile.

[‡] Department of Chemistry, Faculty of Physical and Mathematical Science, University of Chile.

[§] Department of Biology, Faculty of Science, University of Chile.

10.1021/bm0055091 CCC: $19.00
Published on Web 04/27/2000

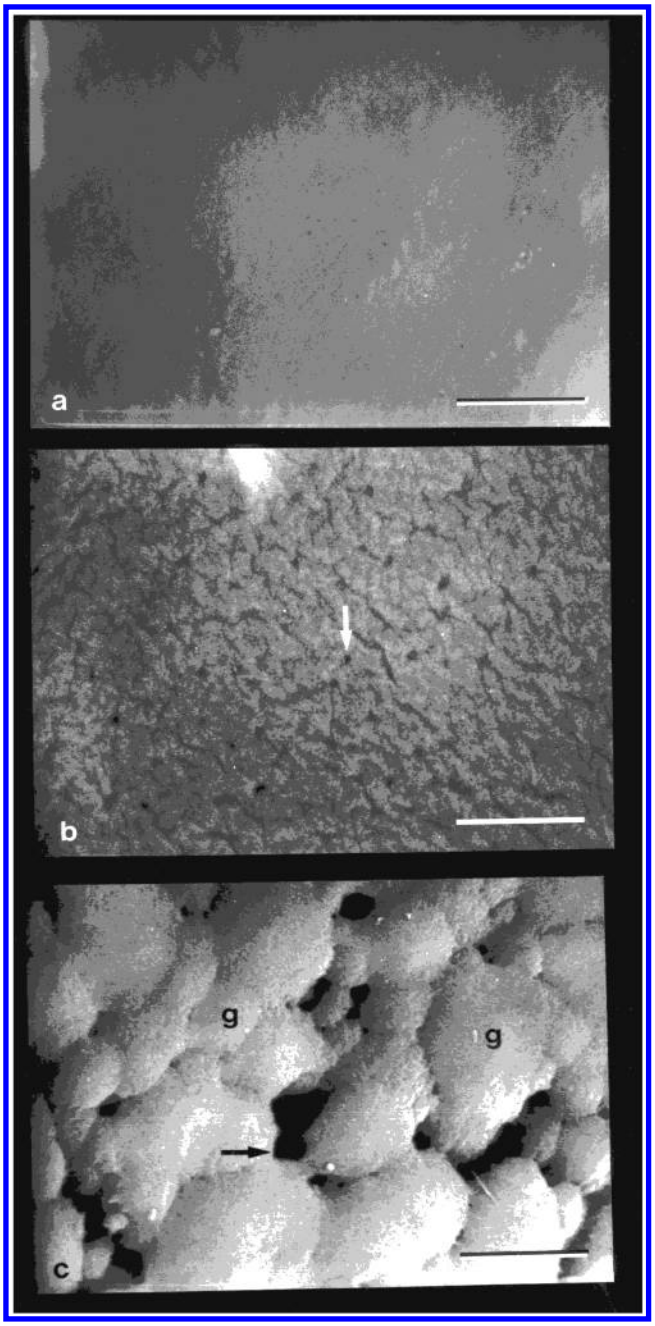

Figure 1. SEM micrographs: (a) chitosan (CHI) film, (b) poly(aminopropylsiloxane) (pAPS) film, and (c) CHI/pAPS (0.6:1 ratio molar) complex film. Pores are indicated by arrows. g: globules. Magnification bar: 10 μm.

lithium perchlorate (Merck) was added as a 1 M solution in absolute ethanol. Further addition of lithium perchlorate led to formation of opaque, nonhomogeneous films due to crystallization of the salt into separate domains.

Film Preparation. CHI and pAPS solutions in the appropriate ratios were stirred for about 24 h at room temperature. Films were then prepared by solution casting on a polypropylene film, after letting the solvents to evaporate at room temperature. Depending on the solution concentration, 50−100 μm thick films were obtained. Films were characterized by simultaneous thermal analysis, DSC/TGA (STA625, Polymer Laboratories); FT-IR spectroscopy (Perkin-Elmer 2000); X-ray diffraction analysis (Siemens D-500); scanning electron microscopy (Philips EM 300); and video-enhanced differential interference contrast (VEC-DIC) microscopy.

Results and Discussion

Scanning Electron Microscopy. Films obtained from a 0.6:1 molar ratio CHI/pAPS mixture were flexible and transparent, indicating compatibility of the components at the molecular level. Scanning electron micrographs of CHI, pAPS, and CHI/pAPS (0.6:1 molar ratio) films are compared in Figure 1. As seen in Figure 1a, the surface of CHI films had a smoothed and more uniform surface that the other films (compared with parts b and c). Pores were not detected. Their texture is clearly smooth. In the case of pAPS films (Figure 1b), the precursor solution contained low molecular weight oligomers that led to the formation of films with corrugated surface. These films displayed some pores (pore diameter < 1 μm) but no others distinctive structural features. As can be seen in Figure 1c, CHI/pAPS films exhibited different structural features. Globular elements, about 20 μm in diameter, were distinguished. Moreover, the arrangement of these elements gave rise to rounded or irregularly shaped mesopores of about 5 μm in diameter.

The morphological properties of the hybrid films described here point toward a structural ordering created by the molecular affinity among their components. In this manner, a new complex phase or an orderly arrangement of two or more phases is formed. The molecular interactions engaged in such structures should also be reflected in other macro- and microscopic properties of the films. Thereafter, noticeable differences between the properties of hybrid films and those of their parent components were expected. This indeed was observed when the thermal stabilities of the above-mentioned types of films were compared.

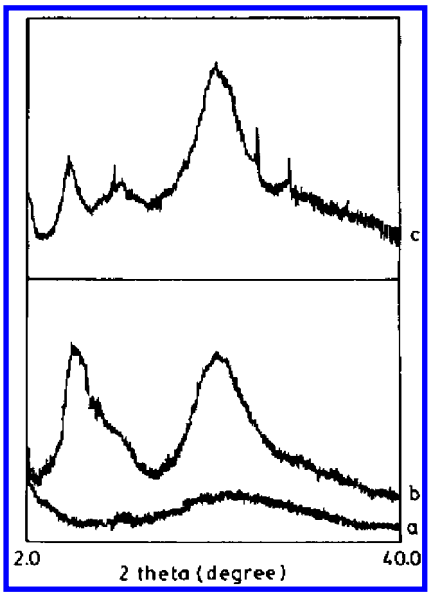

Figure 2. X-ray diffraction spectra of films: (a) CHI, (b) pAPS, and (c) CHI/pAPS (0.6:1 molar ratio).

Table 1. Percentage of Weight Loss at 550 °C of Chitosan (CHI), Poly(aminopropylsiloxane) (pAPS) and CHI/PAPS (0.6:1 Molar Ratio) Complex, As Measured by Thermogravimetric Analysis (TGA)

sample	weight loss, %
CHI	70
pAps	30
CHI/pAPS	60

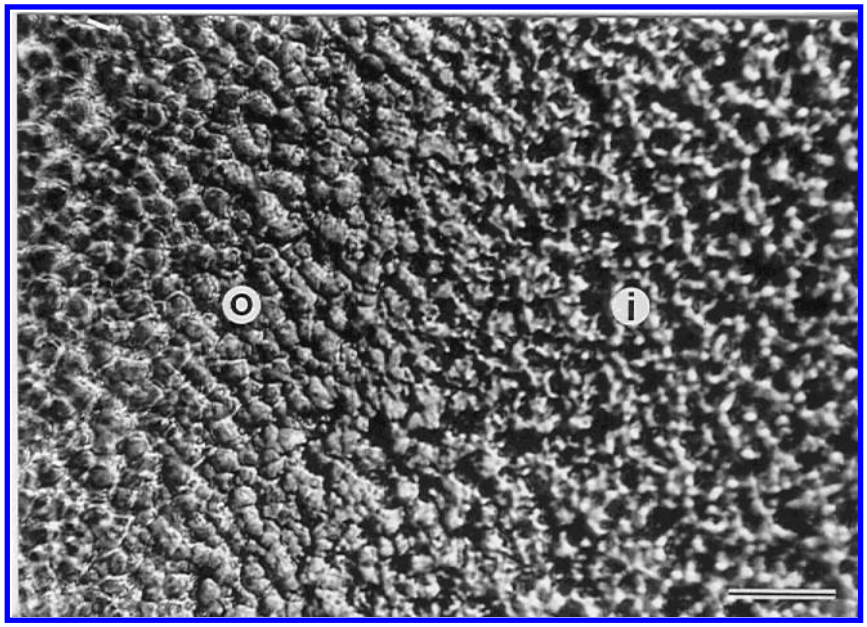

Figure 3. VEC-DIC micrograph of CHI:pAPS (0.6:1 molar ratio) film: (a) outer layer (○) and (b) inner layer (i). Magnification bar: 40 μm.

Thermal Analysis. As previously reported,[14] the simultaneous thermal analysis (DSC/TGA) of CHI/pAPS (0.6:1 molar ratio) films showed only one decomposition peak. That is in contrast with the thermograms of mixtures with other molar ratios, where peaks assignable to each of the components were always observed. This confirms that for CHI/pAPS (0.6:1 molar ratio) solutions the blend behaved as a single phase that could be regarded as an interpolymeric complex. However, as will be discussed below, the molecular interactions giving rise to such uniform thermal behavior appeared to be the result of an orderly association of the component domains. Hence, these films may be considered nanocomposites. The decomposition temperature of the nanocomposite is 361 °C. This temperature is intermediate between the decomposition temperature of chitosan (301 °C) and that of pAPS (438 °C), determined under the same conditions. Particularly interesting are the TGA patterns. As can be seen in Table 1, the weight loss of the hybrid film at 550 °C was approximately 60%. That is significantly higher than the 45% weight loss that would correspond to the sum of the contributions from the components. This last value was calculated from the molar ratios, considering the residual weights determined after TGA analysis of films of each component.

X-ray Diffraction Analysis. As discussed above, microscopic studies indicated that nanocomposites formed highly organized films displaying structural patterns different from those of their components (Figure 1). In contrast, X-ray diffraction patterns of the hybrid samples (Figure 2) appeared as superimposed images of each of the pure components. Chitosan diffractograms (Figure 2a) showed only two broad peaks of low intensity, as expected for a rather amorphous substrate. On the other hand, the pAPS diffractogram (Figure 2b), showed well-defined peaks, proper of a more structured material. Indeed, the superposition of both diffractograms (Figure 2c) showed a pattern similar to those observed in the nanocomposite CHI/pAPS (0.6:1 molar ratio). This means that the component domains were sufficiently large to be detected by X-ray diffraction. Considering the nanocomposite nature of the hybrid films, as revealed from thermal analysis, and the existence of separate phase domains, as shown by X-ray diffraction, nanocomposites may be considered to be layered structures.

The existence of such extended ordering of component domains is supported by preliminary results obtained by video-enhanced differential interference contrast microscopy (VEC-DIC). This type of microscopy not only allowed contrast improvement but also increased resolution. As can be seen in Figure 3, the CHI/pAPS (0.6:1 molar ratio) film consisted of outer and inner layers. Globules that fit in pits of the inner layer formed the outer layer. The latter constituted an egg-box-like structure. A systematic study of these films by VEC-DIC microscopy is currently under study.

FT-IR Analysis. Further information on the molecular interactions between the component microdomains and those generated at the corresponding interfaces between themselves, could be obtained by spectroscopic vibrational analysis. Samuels[18] and Urbanczyck[19] have shown that some prominent features observed in the FT-IR chitosan spectra may be related to the crystalline structure of a particular sample. Indeed, they have identified two principal forms of chitosan: an "amorphous" (β) form and a crystalline (α) form. The β-form showed two absorption bands at 1350 and 1380 cm^{-1} and a third characteristic band at 760 cm^{-1}. The α-form, on the other hand, had a peak at 1380 cm^{-1}. At lower frequency the absorption was shifted to 800 cm^{-1}. In this manner, FT-IR allowed to follow the gradual transformation of the β into the α form. The bands at 1350 and 1380 cm^{-1} seemed to arise from stretching vibrations of the methyl group present in the ca. 12% residual acetamido groups of the chitosan, due to incomplete deacetylation of the parent chitin. It is well-known that the band at 1350 cm^{-1}, assigned to the vibrations of the amide$-CH_3$ group, is strongly influenced by groups in its vicinity. Specifically, its degree of freedom can be influenced by intermolecular hydrogen-bonding interactions. Thus, in chitosan samples

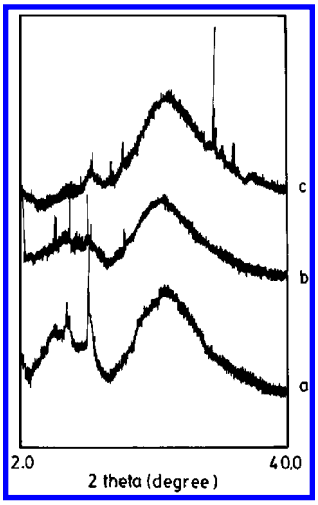

Figure 4. X-ray diffraction spectra of films: (a) CHI/pAPS/$LiClO_4$ (0.6:1:0.1 molar ratio), (b) CHI/pAPS/$LiClO_4$ (0.6:1:0.5 molar ratio), and (c) CHI/pAPS/:$LiClO_4$ (0.6:1:0.8 molar ratio).

with high crystallinity (α-form) this band practically disappears. In the case of the nanocomposite CHI/pAPS the FT-IR spectra also showed two absorption bands at 1350 and 1380 cm^{-1}. These bands were slightly shifted at lower frequencies by 5 cm^{-1}. However, in this case the band at 1350 cm^{-1} showed higher intensity, indicating that the −OH and $-NH_2$ groups of chitosan were not involved in the intermolecular interactions affecting the residual CH_3−amide groups. In other words, the residual amide groups would not be involved in the intermolecular CHI/pAPS connectivity that led to the observed components compatibility. However, the amide groups participation in CHI/CHI macromolecular interactions into the organic domains cannot be discarded.

Effect of the Lithium Ion. As was already mentioned, the DRX spectrum of the CHI/pAPS hybrid film contains the characteristics peaks of both components. Surprisingly, the addition of lithium perchlorate, even in small quantities, notoriously affected the crystalline structure of CHI/pAPS films. Thus, monitoring the effect of the lithium salt by X-ray diffraction showed that, by incorporating growing amounts of lithium salt into the hybrid films (Figure 4, parts a−c), the most notorious change corresponds to the characteristic maxima of the pAPS films located at the lower 2θ region which diminishes progressively. Meanwhile, the maxima located around $2\theta = 24°$ show a small shift to lower 2θ values. Such changes in the diffractograms could be interpreted as a new organization of the complex structure due to the participation of functional groups in coordinating Li^+ ions.

A reorganization of the complex structure of CHI/pAPS nanocomposite was further supported by a notable morphological change in the surface of the films. SEM allowed observing the effect of lithium perchlorate on the structure. As shown in Figure 5, lithium ions transformed the film globular pattern into a smoother pattern. Changes in the microscopic organization of the films induced by lithium ions were also detected by FT-IR spectra. The two most important of these changes were as follows: (1) the gradual decrease, until almost disappearance, of the absorption band at 1350 cm^{-1} and (2) the simultaneous shift of the absorption from

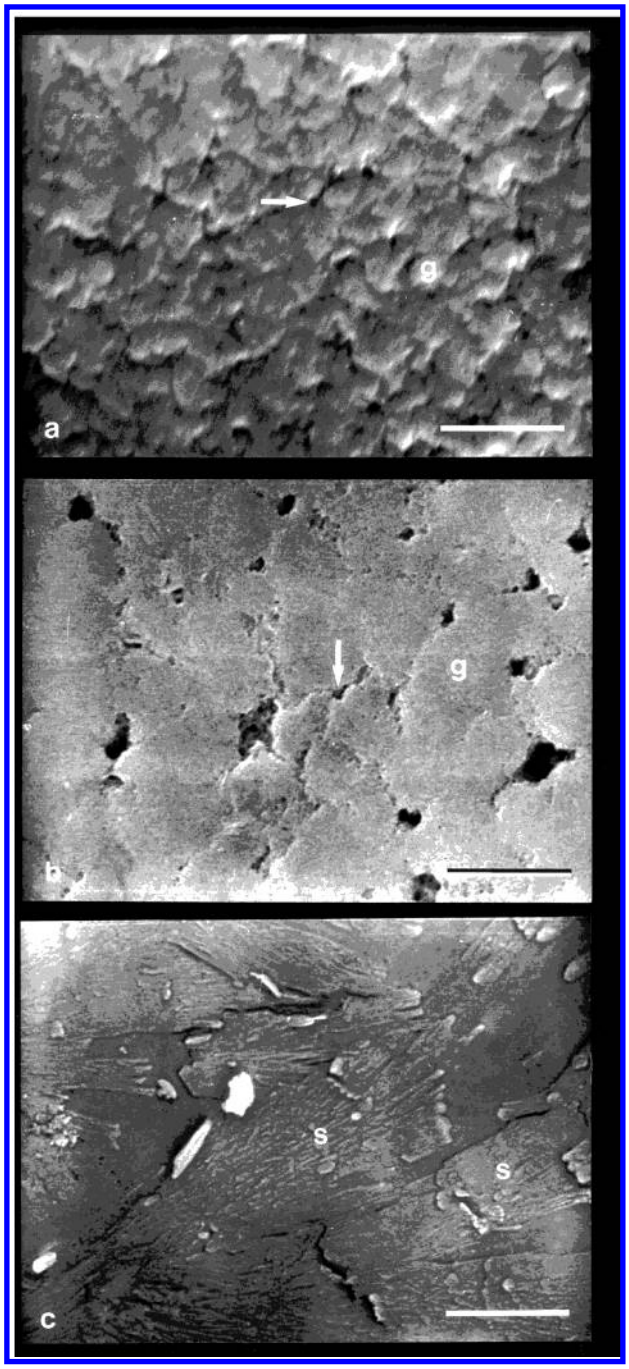

Figure 5. SEM micrographs of films prepared with increasing concentrations of $LiCLO_4$: (a) CHI/pAPS/$LiClO_4$ (0.6:1:0.1 molar ratio), (b) CHI/pAPS/$LiClO_4$ (0.6:1:0.5 molar ratio), and (c) CHI/pAPS/$LiClO_4$ (0.6:1:0.8 molar ratio). Notice that globules turned into scale-like structures (s). Pores are indicate by arrows. g: globules. Magnification bar: 10 μm.

760 to 800 cm^{-1} (Figure 6, parts a−c) with the growing addition of salt. As discussed above, these results may be interpreted as the result of a gradual transformation of chitosan from the β-form into the α-form. The X-ray diffraction and SEM results presented in this paper, wherein lithium is shown to modify the structure of the nanocomposite, support this conclusion. This might be produced by enhancement of the interactions that involve residual amide groups, among chitosan molecules. In this way, the lithium salt appeared to have triggered molecular rearrangements leading to more crystalline forms of chitosan.[18,19]

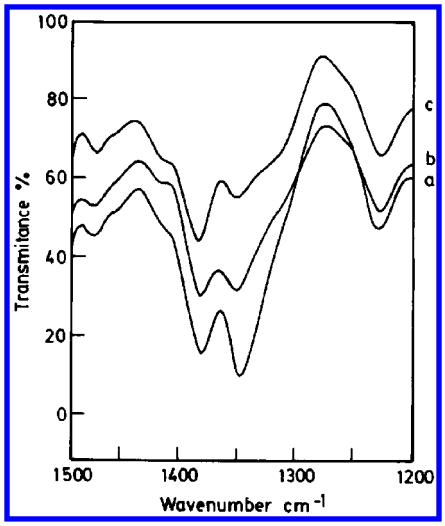

Figure 6. FT-IR spectra of (a) CHI/pAPS/$LiClO_4$ (0.6:1:0.1 molar ratio) film, (b) CHI/pAPS/$LiClO_4$ (0.6:1:0.5 molar ratio) film, and (c) CHI/pAPS/$LiClO_4$ (0.6:1:0.8 molar ratio) film.

Concluding Remarks. The combination of chitosan with poly(aminosiloxanes) in molar ratios of 0.6:1 led to formation of macromolecular aggregates with peculiar properties, different from those of their components. Morphological and spectroscopical studies of films obtained by solution casting revealed that the product is a structured nanocomposite. This self-assembled structure is probably stabilized by intermolecular hydrogen bonding. The incorporation of lithium perchlorate caused important changes in the morphology and crystalline structure of the films, confirming that there must be strong molecular interactions between CHI and pAPS domains. This suggests that both domains are associated in a nanocomposite structure.

Acknowledgment. This work has been financed by Fondecyt (Grants 197-0730, 297-0004, and 1991006), Fundación Andes (Grant C12510), and the University of Chile (DID-CSIC, Spain joined project). We thank the technical assistance of Mr. Víctor Monasterio in electron microscopy. The collaboration of Prof. M. Rinaudo CERMAV-CNRS (Grenoble, France) is greatly appreciated for his help in the characterization of chitosan samples.

References and Notes

(1) Ozin, G. A. *Adv. Mater.* **1992**, *4*, 612.
(2) Chujo, Y.; Saegusa, T. *Adv. Polym. Sci.* **1992**, *100*, 11.
(3) Makishima, A.; Tani, T. *J. Am. Ceram. Soc.* **1986**, *69*, 72.
(4) Levy, D.; Esquivias, L. *Adv. Mater.* **1995**, *7*, 120.
(5) Bandyopadhyay, S.; De, P. P.; Tripathy, P. K. *J. Appl. Polym. Sci.* **1996**, *61*, 1813.
(6) Calvert, P.; Rieke, P. *Chem. Mater.***1996**, *8*, 1715.
(7) Watzke, H. J.; Dieschbourg, C. *Adv. Colloid Interface Sci.* **1994**, *50*, 1.
(8) Kurihara, M. *Pure Appl. Chem.* **1994**, *A31*, 1791.
(9) Schrotter, J. C.; Smaihi, M.; Guizard, C. *J. Appl. Polym. Sci.* **1996**, *61*, 2137.
(10) Muzarelli, R. A. A. *Chitin*; Pergamon Press: Oxford, England, 1977.
(11) Migazaki, M.; Shoso, A.; Yamaguchi, M. *Chem. Pharm. Bull.* **1989**, *36*, 4033.
(12) Rathke, T. D.; Hudson, S. M. *Rev. Macromol. Chem. Phys.* **1994**, *C34*, 375.
(13) Jiang, H.; Su, W.; Caracci, S. *J. Appl. Polym. Sci.* **1996**, *61*, 1163.
(14) Fuentes, S.; Retuert, P.; Gonzalez, G. *Int. J. Polym. Mater.* **1997**, *35*, 61.
(15) Rinaudo, M.; Le Dung, P.; Milas, M. *Int. J. Biol. Macromol.* **1993**, *15*, 281.
(16) Rinaudo, M.; Le Dung, P.; Milas, M. Fr. Patent 9302182, 1993.
(17) Rinaudo, M.; Le Dung, P.; Grey, C.; Milas, M. *Int. J. Biol. Macromol.* **1992**, *14*, 122.
(18) Samuels, R. J. *J. Polym. Sci., Polym. Phys.* **1981**, *19*, 1081.
(19) Urbanczyk, G. W.; Lipp-Symonowicz, B. *J. Appl. Polym. Sci.* **1994**, *51*, 2191.

BM0055091